On the Potential Impact of Modoki El Nino on Atlantic Hurricane Activity

Sarah Larson

Atlantic Oceanographic and Meteorological Laboratory, NOAA, Miami FL

1. Background

Several El Nino Modoki definitions have been referenced in recent literature (Ashok et al. 2007, Yeh et al. 2009, Tranberth and Stepaniak 2001). There is yet a consensus on how to classify El Nino modoki or understanding of the anomaly's variability.

Ashok et al. (2007) generate the ENSO Modoki Index (EMI) to determine modoki years. The index is calculated using the following equation: EMI = SSTA(A) – 0.5*SSTA(B) – 0.5*SSTA(C), where A is the region (10S – 10 N, 165E-140W), B (15S-5N, 110W-70W), and C (10S-20N, 125E-145E). The index is normalized by the standard deviation of the EMI anomaly time series (Ashok et al. 2007).

Yeh et al. (2009) define modoki years using a Central Pacific Warming (CPW) index. The index is calculated by taking the difference between the SSTA of the NINO4 region (5N-5S, 160E-150W) and the SSTA of the NINO3 region (5S-5N, 160E-150W). CPW index is positive when NINO4 SSTA exceeds NINO3 SSTA (Yeh et al, 2009).

Tranberth and Stepaniak (2001) define ENSO with a Trans-Nino index (TNI). TNI is computed by "the difference between the normalized SST anomalies averaged in the Nino-1+2 (0-10S, 80-90W) and Nino-4 regions... we further normalize the resulting series to have unit standard deviation" (Tranberth and Stepaniak 2001). The resulting TNI is a SSTA gradient between the NINO1+2 and NINO4 regions (Tranberth and Stepaniak 2001).

2. Data

The data set used in this study is the NOAA Extended Reconstructed Sea Surface Temperature version 3 (ERSST3) from January 1871 through December 2008. ERSST3 has a horizontal grid resolution of 2 X 2.

SSTA are calculated for 40S-40N and are referred to as TropSSTA hereafter. The 3-month seasonal averages of TropSSTA for DJF, FMA, AMJ, JJA, ASO, and OND are computed for the time series. The NINO3 index is computed for the time series to compare with modoki indices.

In this study, the EMI, TNI, and CPW methods are each applied to the ERSST3 data set

The TNI and CPW indices are modified for the purpose of this study. To compute the TNI, the normalized NINO1+2 SSTA is subtracted from the normalized NINO4 SSTA. This way a positive TNI index corresponds to a modoki year. A recent study by Kim et al. (2009) argued that the magnitude of Eastern Pacific Warming (EPW) is larger than CPW. Therefore, in this study the CPW index is computed by taking the difference between the normalized SSTA of NINO4 and the normalized SSTA of NINO3. The CPW is further normalized by the standard deviation of the time series. This way all three indices can be compared by unit standard deviation.

3. Modoki Indices

Figure 1 (a-d) shows a time series of the El Nino modoki indices and the canonical EL Nino index (NINO3). Generally, the modoki indices are in agreement but highly variable in the first two decades. TNI and EMI are in closest agreement with phase, duration, and intensity.

The CPW appears the least favorable modoki index. The CPW index compares NINO3 SSTA and NINO4 SSTA but does not taken into account extreme Eastern Pacific SSTA as do the TNI and EMI indices. Disregarding the first two decades in which all three indices show disagreement, significant phase disagreement of CPW with the TNI and EMI occur from 1890s-1910s and 1930s-1940s. The consensus between TNI and EMI time series makes CPW appear an outlier. Therefore, regressions of the indices onto SSTA, vertical wind shear, and Convective Available Potential Energy

(CAPE) are calculated and plotted to compare the different indices. NINO3 index is also calculated and plotted to further compare modoki to the canonical El Nino.

4. Methodology

The Central Pacific Warming (CPW) Index is the difference between the SSTA of NINO4 and SSTA of NINO3 (Yeh et al. 2009). For this study, both SSTA of NINO4 and SSTA of NINO3 are normalized by the respective standard deviation of the anomaly time series. Similar to Yeh et al. procedure, the CPW index is further normalized by the standard deviation of the time series. A time series from January 1871 through December 2008 of monthly CPW index is plotted. The 3-month seasonal averages for DJF, FMA, AMJ, JJA, ASO, and OND are then computed for the time series.

The CPW index seasonal averages are regressed onto the respective TropSSTA seasonal averages and plotted for the 40S-40N ERSST3 grid. The most distinct maximums are seen in DJF and FMA in the Central Pacific from 160E-140W with FMA being the relative maximum of all seasons. Greatest values are seen along the equator near the dateline then extending northeastward. That being said the magnitude of warm SSTA is noticeably less than EMI and TNI. Distinct minimums are seen from JJA through OND along the equator from the west coast of South America extending westward. During ASO, only a slight maximum is seen near the dateline/equator intersection with another to the northeast. Pronounced cool SSTA in Eastern Pacific is the dominant feature. The tropical North Atlantic remains neutral except for a slight maximum seen in FMA and AMJ. CPW index appears to be linked more distinctively with an Eastern Pacific cooling trend than pronounced Central Pacific warming. The CPW SSTA structure resembles La Nina.

Tranberth and Stepaniak (2001) define ENSO, characteristically Eastern Pacific SSTA, with the Trans-Nino Index (TNI) as the normalized SSTA of NINO4 subtracted from normalized SSTA of NINO1+2. However, for the purpose of this study, warm Central Pacific SSTA is calculated as the normalized SSTA of NINO1+2 subtracted from normalized SSTA of NINO4. The resulting TNI is

further normalized by the standard deviation of the anomaly time series. 3-month seasonal averages are calculated for the time series. A time series from January 1871 through December 2008 of monthly TNI is plotted as well as the seasonal averages regressed onto the respective TropSSTA seasonal averages.

The regression plot of TNI onto TropSSTA shows a different seasonal distribution than the CPW index. The relative maximum is seen in DJF in the Central Pacific extending along the equator from 165E-115W. Additional warm Central Pacific SSTA are seen in FMA, ASO, and OND. Greatest cool SSTA are seen in AMJ, JJA, and ASO extending from the west coast of South America along the equator. However, the minimum SSTA do not extend as far west as CPW minimum SSTA. TNI shows strong minimums off the west coast of South America along the equator in AMJ and JJA. The warm Central Pacific SSTA does not appear as strong as CPW and EMI in AMJ and JJA. IN ASO, TNI shows two separate warm SSTA in the Central Pacific and cool SSTA off the west coast of South America, similar to the CPW ASO pattern but more distinctive. The tropical North Atlantic shows a slight warm SSTA in FMA but remains neutral for the other seasons.

Ashok et al. (2007) classify Modoki years by the ENSO Modoki Index (EMI) which takes into account Eastern, Central, and Western Pacific SSTA. EMI is found by subtracting ½ SSTA in the Eastern Pacific (15S-5N, 110W-70W), and ½ SSTA in the Western Pacific (10S-20N, 125E-145E) from SSTA in the Central Pacific (10S – 10 N, 165E-140W) (Ashok et al. 2007). The EMI is further normalized by the standard deviation of the time series (Ashok et al. 2007). 3-month seasonal averages are calculated for the time series. A time series from January 1871 through December 2008 of monthly EMI is plotted as well as the seasonal averages regressed onto the respective TropSSTA seasonal averages.

The regression of seasonal EMI onto TropSSTA shows less seasonal variability than CPW and TNI. Warm Central Pacific SSTA are found along the equator in all seasons with strong maximums seen in DJF (greatest), FMA, ASO, and OND. Distinctive cool Central Pacific SSTA are seen in AMJ

and JJA only and appear weakest of the three indices. Strongest warm SSTA are located at the equator but the warm anomaly extends moderately to the northeast during all seasons. Similar to CPW and TNI, a slight warm SSTA appears in the tropical North Atlantic but disappears in the other months.

5. Indices and Vertical Wind Shear

The vertical wind shear regression patterns in figures 6-9 (a) show CPW as an obvious outlier during August-October. Generally, NINO3, EMI, and TNI associate a positive index with an increase in vertical wind shear (VWS) in the MDR while CPW shows neutral to decreasing VWS. Positive EMI and TNI suggest modoki-driven VWS anomalies might hinder hurricane activity in the tropical North Atlantic.

The regression patterns for NINO3 and EMI in the Atlantic are agreeable. Both show a similar association between positive index and VWS response from 10S-25N, however the magnitude of NINO3 anomalies are stronger. The overall CPW pattern looks nearly opposite the NINO3 and EMI. The TNI pattern does not resemble the NINO3/EMI or CPW entirely but rather a mixture of the two. The modoki indices do not agree in VWS response in the Eastern Pacific around 10N. Positive CPW/TNI (EMI) is associated with an increase (decrease) in VWS. Strong negative anomalies are seen from 0-20N in the Eastern Pacific in both NINO3 and EMI. The TNI positive anomaly is flanked by negative anomalies to the north and south. Therefore, it is difficult to hypothesize how modoki-driven vertical wind shear anomalies might impact the hurricane activity in the Eastern Pacific.

6. Indices and CAPE

Looking at figures 6-9 (b), all three modoki indices display a similar Convective Available Potential Energy (CAPE) regression pattern during August-October. The 60W line appears to be a transitional zone between positive and negative CAPE regressions for all modoki indices. East of the 60W line, positive modoki indices are associated with negative CAPE anomalies. West of the 60W

line, positive modoki indices are associated with positive CAPE anomalies. [?? This may be associated with the location of the subtropical high in the North Atlantic. Perhaps the subtropical high is enhanced during modoki years. We expect subsidence (negative CAPE anomalies) on the east side of the subtropical and lifting (positive CAPE anomalies) on the west side of the subtropical high. If the high was stronger than climatology then we might see this CAPE regression pattern ??] Positive CAPE anomalies in the Caribbean are strong when EMI and TNI are positive.

EMI and TNI are in consensus with CAPE response in the Gulf of Mexico. Both indices associate positive index with strong positive CAPE anomalies while CPW remains fairly neutral.

There is a discrepancy in the CAPE response from 0-20N in the Eastern Pacific. TNI and CPW show a positive index is associated with negative CAPE anomalies from 0-10N and a transition from negative to positive anomalies from 10-20N. EMI shows a positive index is associated with neutral or positive CAPE anomalies from 0-10N and strong positive anomalies from 10-20N.

In summary, when considering only TNI and EMI indices, positive modoki index appears to be associated with strong positive CAPE anomalies in the Caribbean and Gulf of Mexico. It would be interesting to see how CAPE anomalies correlated with track density in this region.

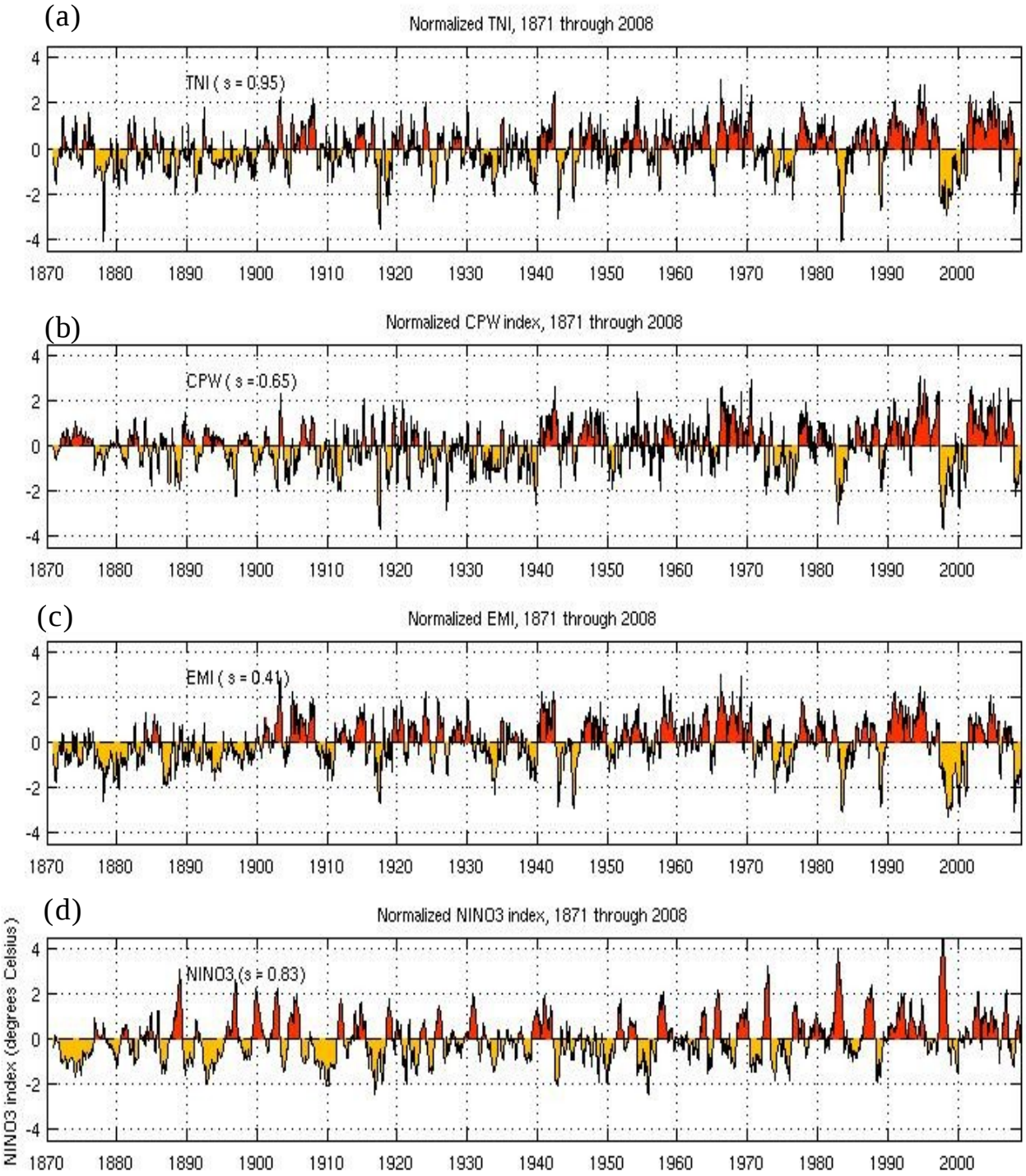

Figure 1. Time series of (a) normalized TNI, (b) normalized CPW index, (c) normalized EMI, and (d) normalized NINO3 index for January 1871 through December 2008.

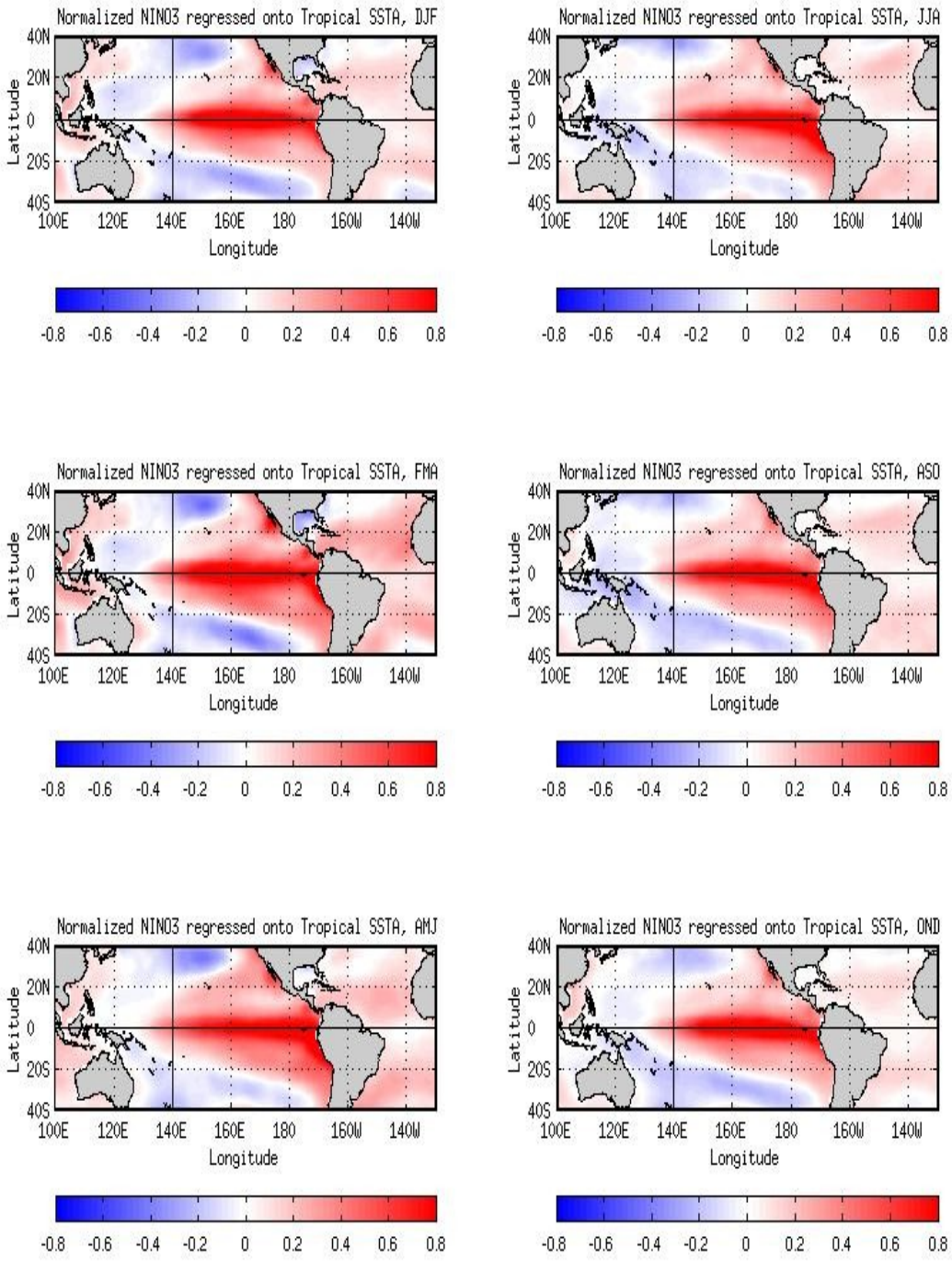

Figure 2. Normalized NINO3 index regressed onto SSTA for seasons DFJ, FMA, AMJ, JJA, ASO, and OND.

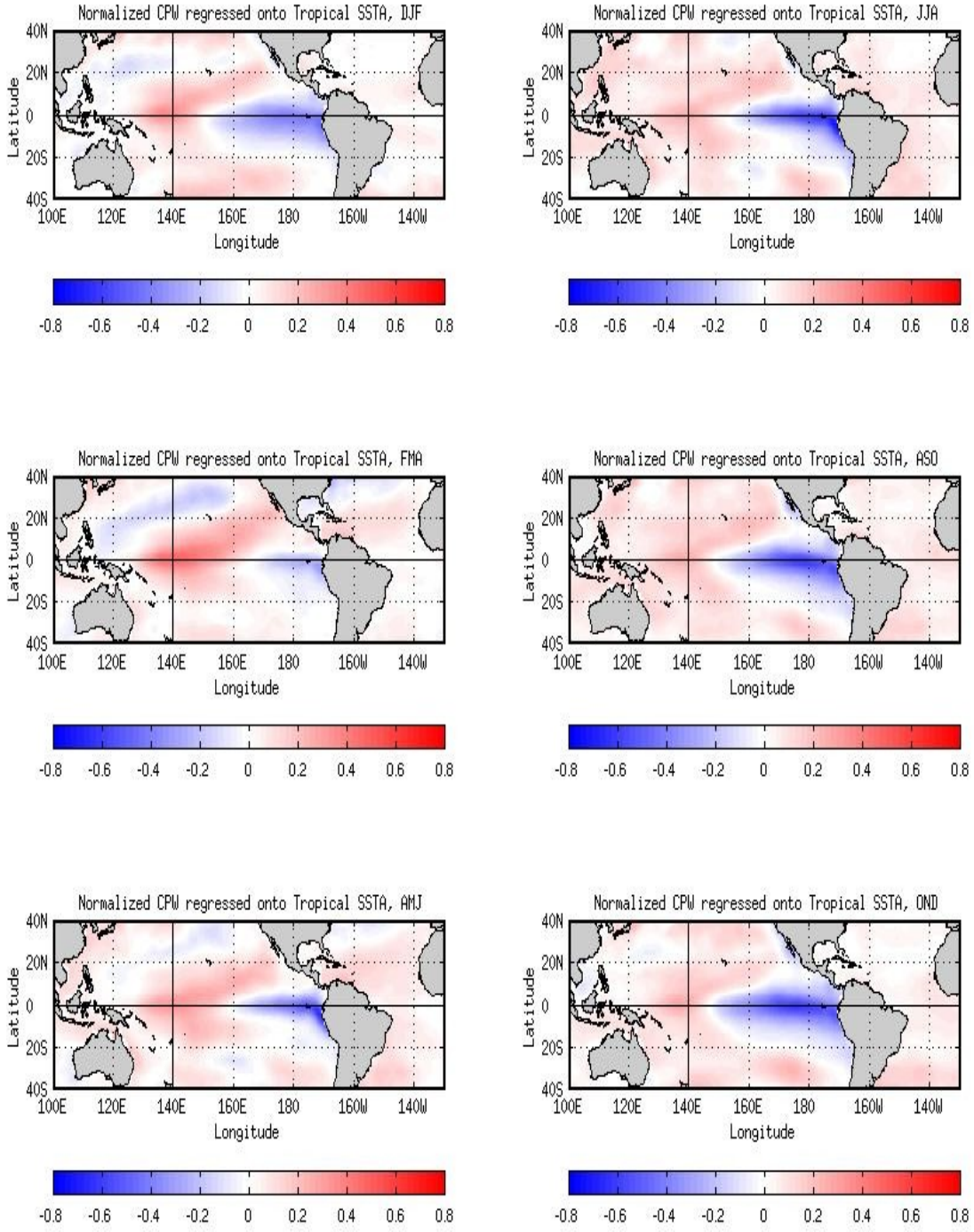

Figure 3. Normalized CPW index regressed onto SSTA for seasons DFJ, FMA, AMJ, JJA, ASO, and OND.

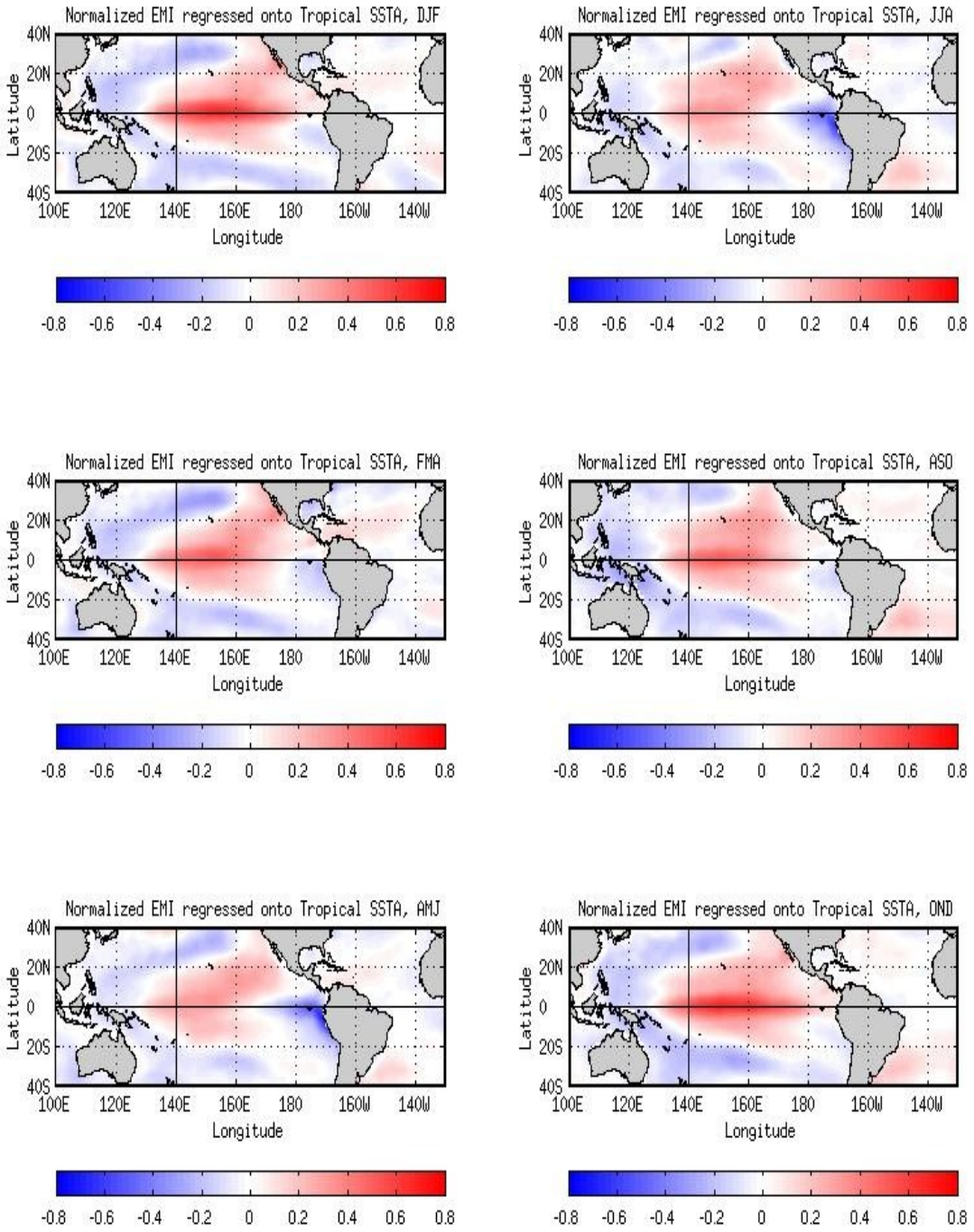

Figure 4. Normalized EMI regressed onto SSTA for seasons DFJ, FMA, AMJ, JJA, ASO, and OND.

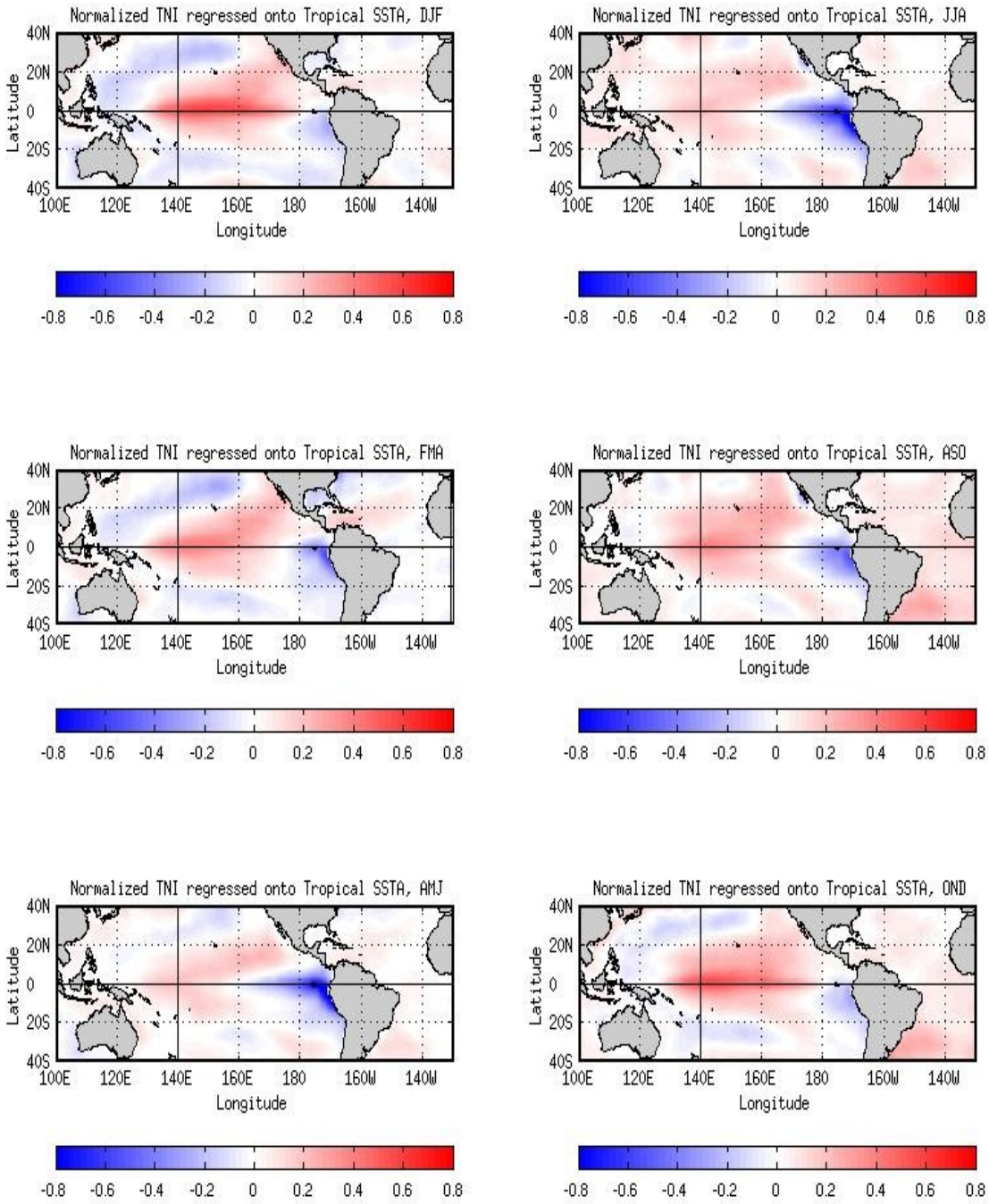

Figure 5. Normalized TNI regressed onto SSTA for seasons DFJ, FMA, AMJ, JJA, ASO, and OND.

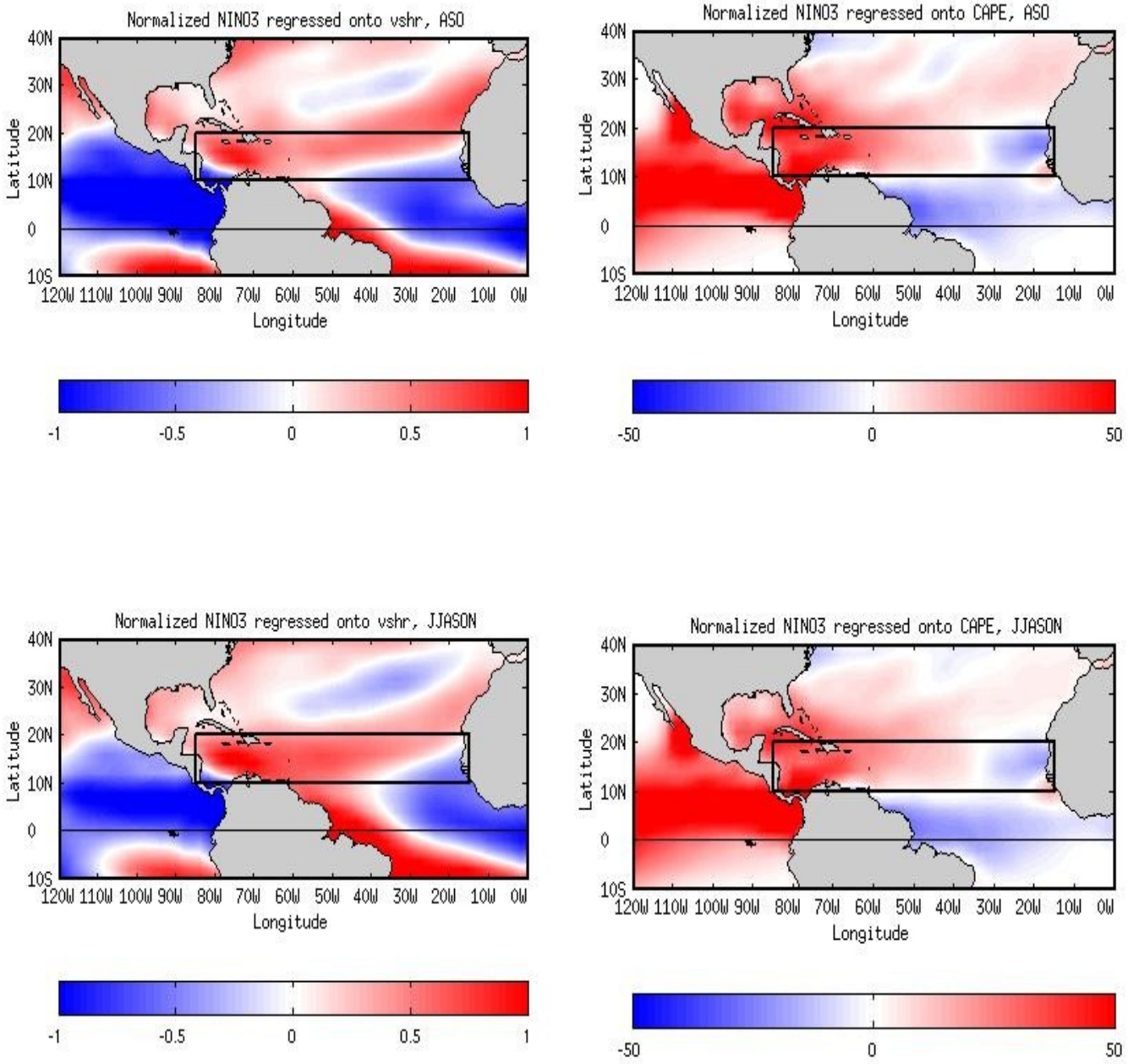

(a) (b)

Figure 6. Normalized NINO3 index regressed onto (a) vertical wind shear (200mb minus 850mb) and (b) CAPE for ASO (top) and JJASON (bottom).

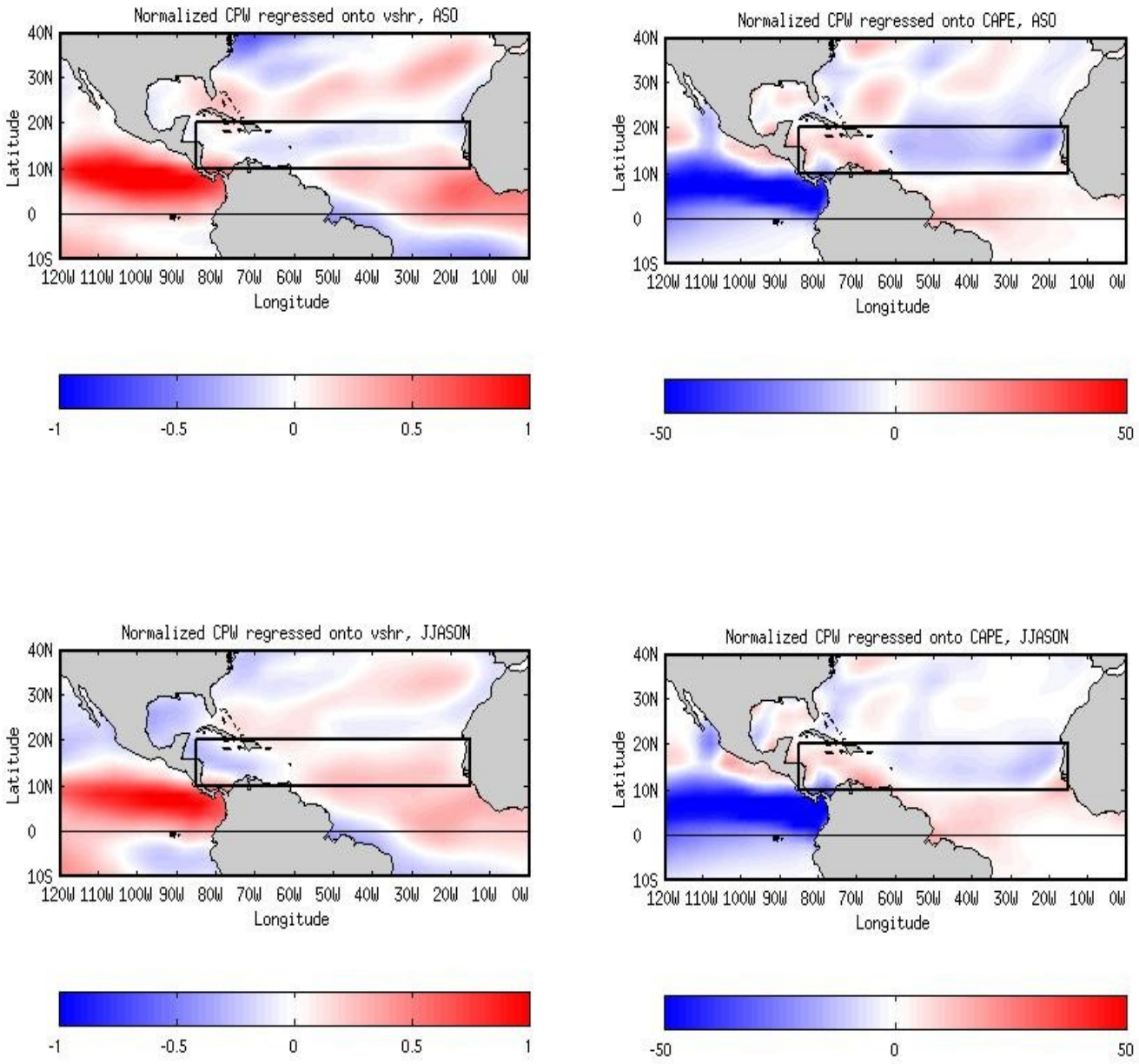

(a) (b)

Figure 7. Normalized CPW index regressed onto (a) vertical wind shear (200mb minus 850mb) and (b) CAPE for ASO (top) and JJASON (bottom).

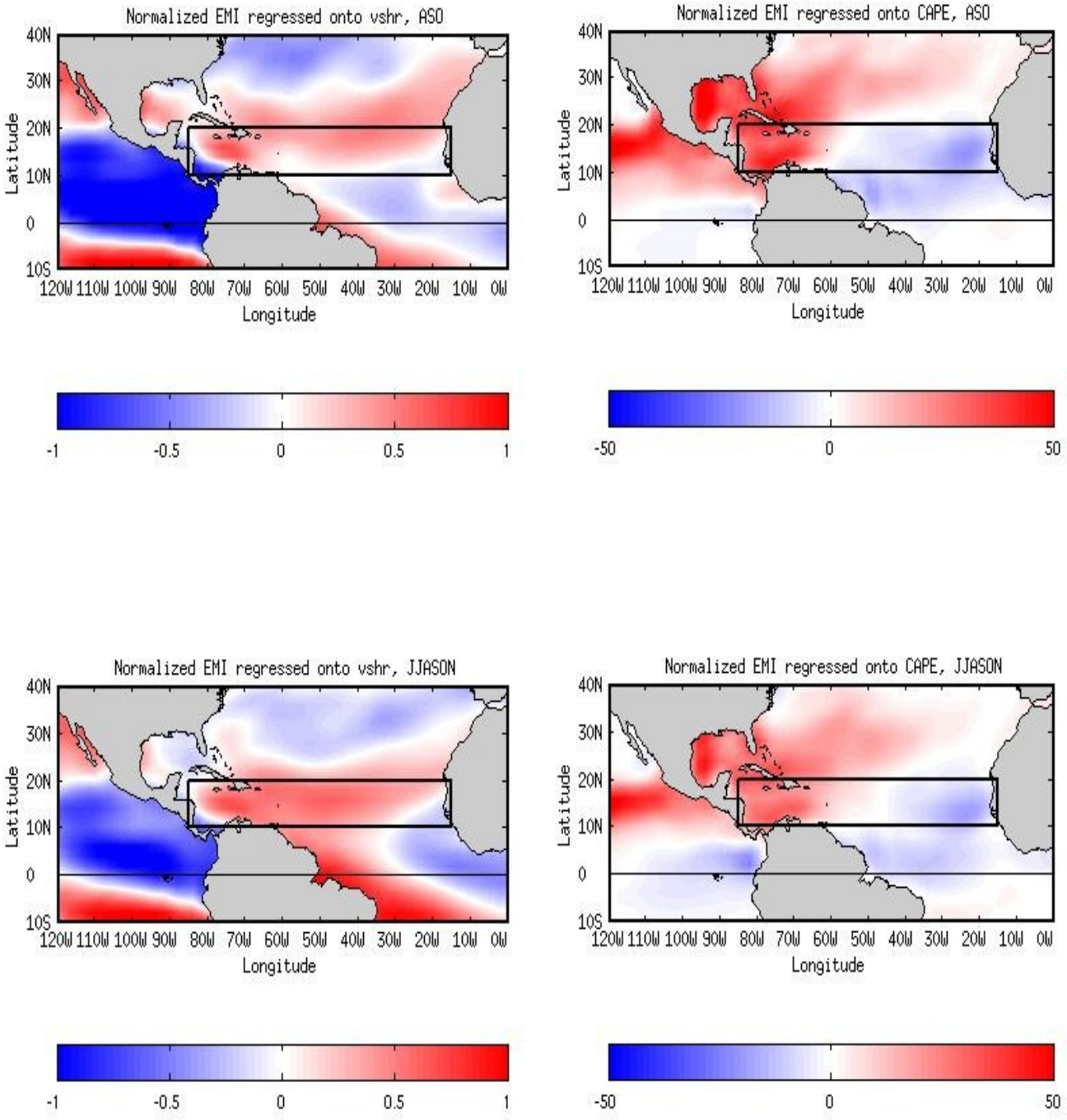

(a) (b)

Figure 8. Normalized EMI regressed onto (a) vertical wind shear (200mb minus 850mb) and (b) CAPE for ASO (top) and JJASON (bottom).

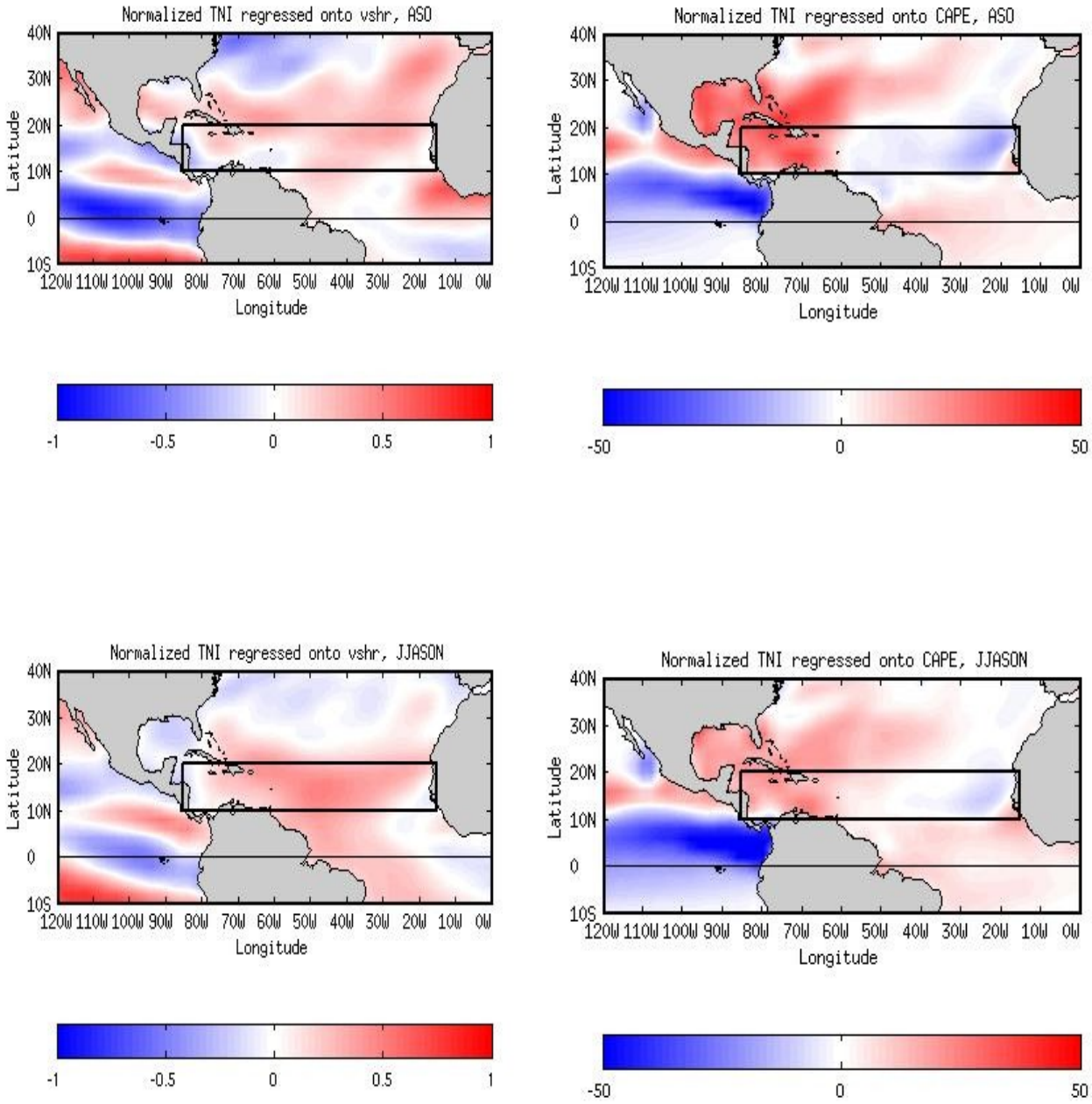

(a) (b)

Figure 9. Normalized TNI regressed onto (a) vertical wind shear (200mb minus 850mb) and (b) CAPE for ASO (top) and JJASON (bottom).